Hydrodynamic response of an ROV during launch and recovery

Clandia Sim, Newcastle University, UK
Bingbing Ke, Newcastle University, UK
Kang Tay, Newcastle University, UK
Musa Bashir, Newcastle University and SMD Ltd, UK
Simon Benson, Newcastle University, UK

The prediction of wave-induced loads on Remotely Operated Vehicles (ROV) during deployment through the splash zone is an important requirement to the design of a launch and recovery system. However, current industry practice and corresponding classification rules only give very basic and sometimes overly conservative safety factors as a basis for handling system design. There is need to develop a better understanding of the behaviour of the ROV as it enters and leaves the water, particularly in high sea states. This will improve the design of the handling system and give better guidance to ROV operators when launching vehicles in severe sea environments. To improve the understanding of ROV hydrodynamics during launch and recovery, a series of experimental tests have been carried out by marine technology students at Newcastle University. The experiments link to an industry sponsored Knowledge Transfer Project (KTP) which is ongoing between the university and Soil Machine Dynamics Ltd. The experiments have been completed in the hydrodynamic labs at Newcastle University. A scaled model of a cable trenching ROV has been tested in a variety of configurations whilst being raised and lowered through the water surface. Tests in calm water, regular and irregular waves have been completed. The effects of geometry, buoyancy distribution, winch wire stiffness, lifting speed and wave frequency on the motion of the ROV and the lifting line forces have been evaluated. The results show the different factors of influence which must be considered when predicting the maximum winch line load during launch and recovery of an ROV. The results are useful for validating equivalent numerical calculations and for the development of new design methods for ROV handling systems.

1. Introduction

Remotely operated vehicles (ROV) are essential tools used in the development and exploration of seabed resources. This includes mining seabed minerals, servicing offshore hydrocarbon production facilities and surveying the subsea environment. ROVs are useful for any underwater environment that is beyond human reach.

The deployment and recovery of ROVs from the seabed are normally completed using a combination of winches (with wires) and a handling structure (A-Frame) mounted on a support vessel and a cursor fitted to the winch wires for control purposes. Accurate design of an ROV's launch and recovery system (LARS) is very essential to achieving safe deployment and recovery process and also in minimising the likely occurrence of failure modes like slacking and snatching of the umbilical or tether as the occurrence any of these failures could lead to delays in the entire subsea operations or it might even lead to a total loss of the ROV.

This project investigates the launch and recovery process for an ROV. The aim is to better understand the motion characteristics as the ROV passes through the splash zone and is affected by waves. This study has completed experimental testing in the towing tank at Newcastle University. The study is part

of a wider Knowledge Transfer Project ongoing between Newcastle University and Soil Machine Dynamics Ltd, who are one of the UKs leading ROV manufacturers.

This study has completed three different experiments on a 12th scale model of a large ROV:

- Study One - Investigating the loads and motions of the ROV during recovery in regular waves (led by Clandia Sim)

- Study Two - Investigating the effect of winch wire stiffness' on the ROV motion (led by Kang Tay)

- Study Three - Investigating the damping characteristics of the ROV at different water depths (led by Bingbing Ke)

Study one was completed in March 2015 whilst studies two and three were completed in August 2015.

The outcome of the work is a better understanding of the hydrodynamic behaviour which characterise the ROV when located in the splash zone. Progress is made towards defining hydrodynamic coefficients which can be used in software such as OrcaFlex to better simulate a launch and recovery process.

2. Background

2.1 Launch and Recovery Process

The launch and recovery process can be broken into six stages which are shown in Figure 1 [1]. In this project, we focus on the 'splash zone lowering/recovering' stage. At this stage the ROV is affected by wave motion. The hydrodynamic characteristics of the ROV when entering or leaving the water are complex. The buoyancy, drag, damping and added mass may all be affected by the relative position of the ROV to the water surface.

2.2 Experimental Tests

There are limited previous attempts to model the launch and recovery of an ROV in laboratory conditions. Sayer [2] undertook an experiment to measure wave forces on an 1/8 scale model of a ROV and compare results against a numerical method. The conclusion is the combination of simple linear theory using total derivatives together with taking Morison coefficient $Cm\approx1.5$ to give a reasonable estimation.

The experiments were conducted in a 93m x 7m x 2.2m tank. The deep-water criterion was satisfied. A full-scale wave period between 5s and 12s with wave heights up to 5m was selected to satisfy $0.025<H/\lambda<0.090$. A simplified 1/8 scale model of Super Scorpio ROV and a square-section rectangular box with the same overall envelope dimension as the ROV model are tested. This covered a range of KC numbers $0<KC<5$. The experiments consist of two parts, one was rigidly hinge the model

above the water and measured the wave force and moments. And the second part was attached a load-cell to the model and measured the movements by a linear voltage displacement transducer. Figure 2 shows the set-up of the facility.

Ongoing work at Newcastle University has completed several experiments on the launch and recovery process, more details can be found in Bashir et al. [3]. The work presented in this paper follows directly from these experiments.

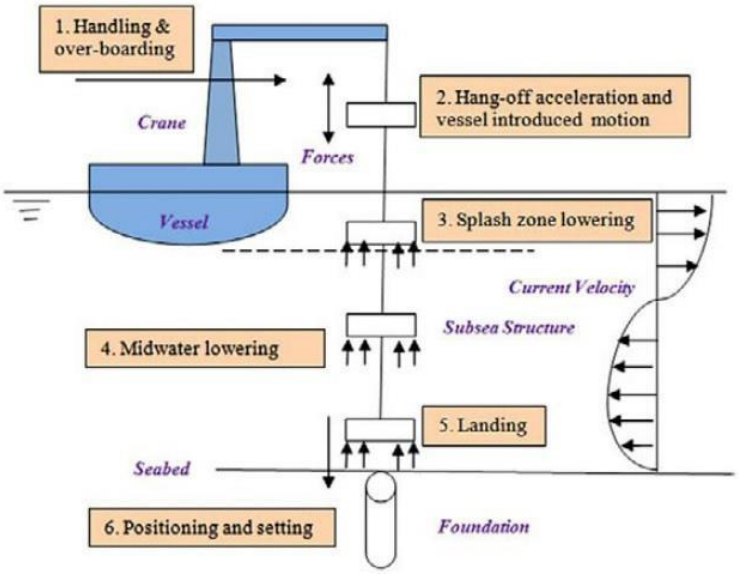

Figure 1. Sketch of analysis steps for typical subsea structure. [1]

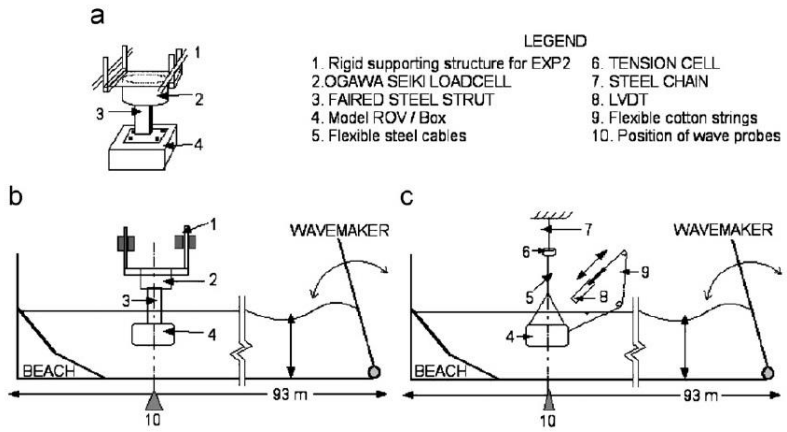

Figure 2. Experiment setup [2]

2.3 Hydrodynamic Coefficients

Design and application of ROVs relies highly on the appropriate selection of the hydrodynamic coefficients, which are the predictions mostly based on assumptions of ideal conditions. OrcaFlex is a widely used software for data analysis in the offshore industry. The accuracy of OrcaFlex simulations depend on the input hydrodynamic coefficients.

In many cases, hydrodynamic forces can be predicted by Morison's Equation using the experimentally determined coefficients (added mass and drag coefficients). This idea of predicting hydrodynamic coefficients by decay tests was brought by Morison and Yoerger [4], where it was proved feasible to determine the coefficients in heave direction. In this experiment, the tested ROV was suspended in the water by three springs which are connected to an overhead crane. A Sonic High Accuracy Ranging and Positioning System (SHARPS) was used to ensure desirable results. The hydrodynamics then can be calculated from the data recorded in the decay test.

Similar experiments were conducted by a group of researchers from School of Mechanical & Aerospace Engineering, Nanyang Technological University (AME, NTU) [5]. In this study, a ROV model was used to determine the hydrodynamics added mass and drag forces. By applying the laws of similitude, the hydrodynamics parameters of the scaled model were then scaled up to predict the corresponding values for the full scale vehicle, and it showed that they closely match with the simulation results from a computational fluid dynamics (CFD) program.

Both methods are used to predict the two important hydrodynamic coefficients related to added mass and drag which are used in Morison's Equation, but the second method is preferred. It is easier and more convenient to do testing using a scaled model instead of the fully scale ROV, and it is more practical when we are able to do predictions on numerical model from scaled model.

Besides mentioned hydrodynamic parameters, damping coefficient is another important factor to the hydrodynamic loads. There is limited data available relevant to damping parameters prediction, but Bashir managed to determine the damping coefficient in his experiment for prediction of hydrodynamic loads. Damping coefficients and other important hydrodynamic parameters were calculated from data of free decay tests [3]

Though Bashir didn't continue to investigate how damping coefficients affects the hydrodynamic loads and motions of the ROV, he proposed a feasible way to achieve this investigation. By this method, added mass and damping coefficient of all the 6 DOF can be calculated and thus can be used as data input in OrcaFlex when doing data analyse and numerical prediction. This method is time-saving and convenient since data of 6 DOF can be collected in one experiment and be investigated separately for each test.

A method of predicting actual loads is also done using DNV Sesam HydroD by Bashir. Added mass, damping and restoring coefficients are all calculated using empirical formulas from the results of decay tests. The coefficients are then used in HydroD, which uses Morison's theory, to predict the response and the heave loads on the ROV. This method has also proved to be successful in predicting both magnitude and trend of the vertical load.

3. Experiment Method

3.1 ROV Model and Overall Experiment Setup

All experiments used a simplified 1:12 scale model of QT (QTrencher) 1400 ROV which still contains basic geometrical features of real QT 1400(Figure 3). Some further experiments were also completed using a simple box model. The dimension of the box model is equivalent to the outer dimension of the ROV model (Figure 4). The experiments were conducted in Newcastle University towing tank with dimensions 37 m x 3.7 m x 1.25 m. A series of vertical load data was collected by 1000 N load cell and several motion data was collected by Qualysis.

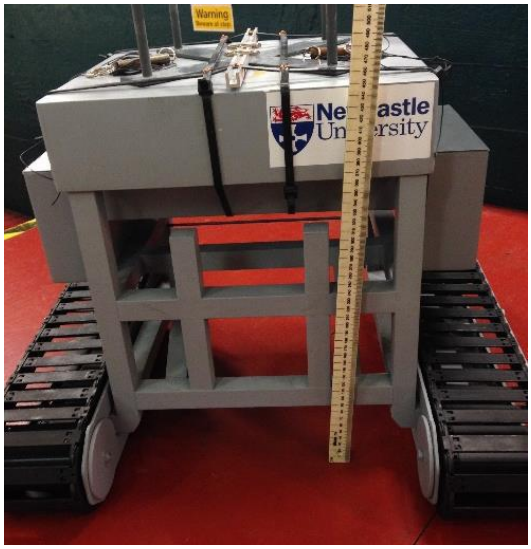

Figure 3. 1:12 scale model of QT 1400.

Figure 4. Box model

3.2 Study One – Recovery Tests

Recovery tests were completed by pulling the ROV out from the water using a constant velocity winch. A winch motor (Clarke CH2500B) was fitted on a beam which leaves an overhead height of 2 m above the waterline. This winch motor provided two constant recovery speeds. And a 3 mm twist free cable was used. The 0.08 m/s recovery speed was set up by double cable and a single cable arrangement is used for 0.16 m/s recovery speed, see Figure 5. Most of the winch properties were taken into account in an equivalent computational model simulated using OrcaFlex software.

Figure 5. The test system setup for two different recovery speed

3.3 Study Two – Winch Wire Stiffness

Motion tests were completed by observing the ROV response when suspended in the splash zone and subjected to different regular wave frequencies. The ROV is suspended using different spring sets on a winch, adjusted to the required submerged height. The 3 spring sets used have 0.4777N/mm, 1.2919N/mm and 2.5182N/mm spring constants. The motion of the ROV is recorded using Qualysis. 10mm amplitude waves were used with frequencies 0.5Hz-1.4Hz. The waves are monitored using a wave probe to account for any inconsistency.

Springs are used with the aim of isolating the ROV from the support wire. This enables direct comparison to motions predicted using a wave diffraction method, such as has been completed by Bashir et al. (2015).

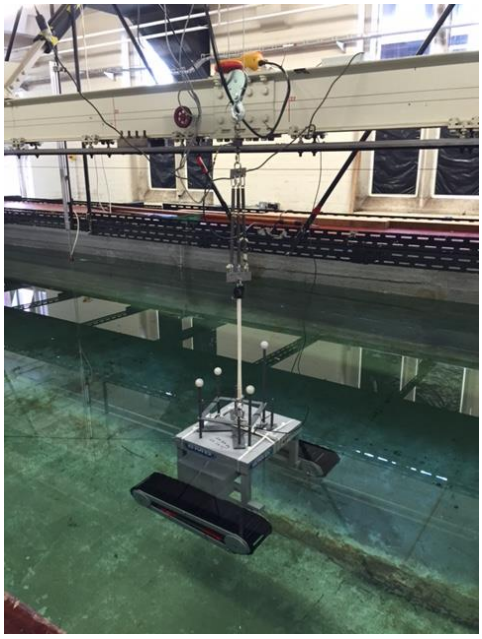

Figure 6. Example spring system setup for ROV model

3.4 Study Three – Damping

Heave decay tests were conducted on both ROV model and box model for different submerged depths with Qualysis balls fitted, which captured the motions of the tested model. The model was put into the towing tank after ballasting in order to meet the desired waterlines when it was stable. A vertical force was then applied on to the model and released to let the tested model free oscillate. Motions of the oscillations were captured and used to calculate the decay rate and model natural period. Tests were repeated several times to ensure accuracy. For ROV model decay test, foams were added to meet some desired waterlines. Five submerged depths for box model and four for ROV model were completed.

Figure 7. Decay tests in different submerged depths of ROV

4. Results

4.1 Study One - Loads and motions of the ROV during recovery

Study one concentrated on the measurement of the vertical load in the winch wire during recovery. We can divide the recovery simulation into 5 main stages, as shown in the table below. All experiment tests were found to exhibit similar trends:

1. There is a peak tension at the start (Stage I) and the end (Stage V) of the recovery.
2. The load increases steadily when the ROV starts to leave the water.
3. The gradient changes in Stage II and III due to the change in geometric shape.
4. The tension fluctuates in small degrees and reduced throughout the whole recovery.
5. The tension fluctuation damps out once the ROV is recovered.

Stage I	The ROV is still fully submerse in the water
Stage II	The buoyancy module is starting come out of the water
Stage III	The tracks are starting come out of the water
Stage IV	The whole ROV is in the air
Stage V	The recovery stopped by the winch motor

Figure 8 plots the tension in the winch wire as a function of time. Recovery simulations were completed in regular wave conditions with wave height 20mm, with a range of frequencies between 0.5Hz and 1.5Hz. The results show that the load was relatively independent from wave frequency.

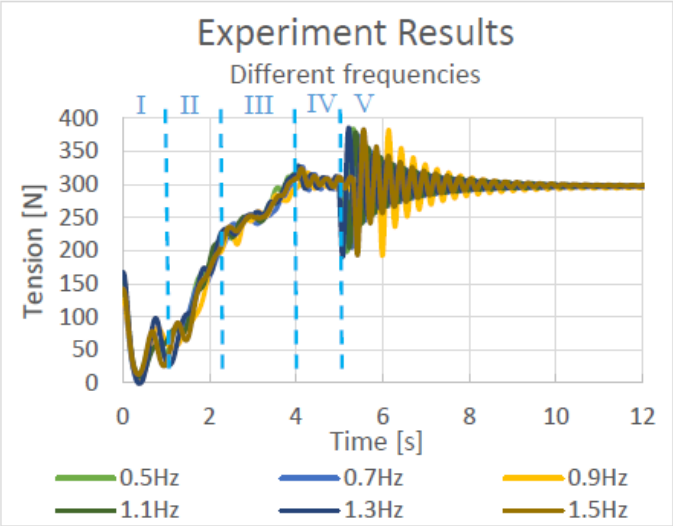

Figure 8. Tension in winch as a function of time for different incident wave frequencies

Figure 9 shows how the load changes in different wave heights. For higher waves, the wire suffered larger fluctuation and peak tension when it is still in the water. The wire was slacking at 0.37 to 0.4 s and experiencing very low tension again at 2.23 s (highlighted in the red box in Figure 7).

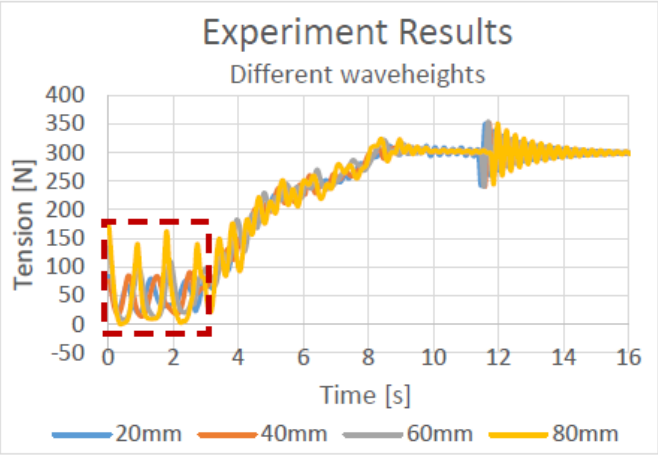

Figure 9. Tension in winch as a function of time for different incident wave heights

The speed of the winch also affects the winch wire loads, as shown in Figure 10 which compares two winch speeds. As the recovery speed increases, there is less tension fluctuation. However, the peak tension at the start of Stage I and V is much higher, due to the higher force required to accelerate the ROV to a higher velocity. Interestingly, there is no slack of wire occurring when increasing the recovery speed.

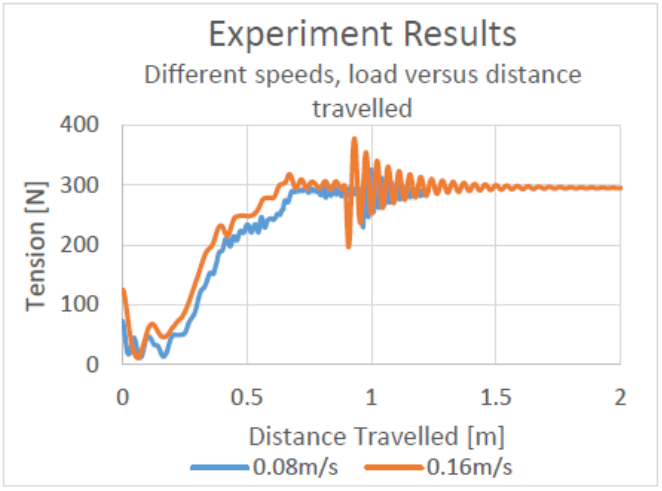

Figure 10. Tension in winch as a function of time for different recovery speeds

Figure 11 compares the experiment, OrcaFlex and a simple hydrostatics calculation of the system at different heights out of the water (and ignoring wave effects). An improved calculation method is also shown in Figure 9. A load response delay of 1 s was added after 3.125 s. It is the time when the ROV is moving out of the water (starting of Stage II). As Figure 9 shows, OrcaFlex gave conservative results, the mean values of both experiment and OrcaFlex results show significate offset, especially in Stage I, II and III. It starts getting under-estimated at the end of stage III. Similar finding were obtained with 0.16 m/s recovery speed. Both experiment and OrcaFlex results are always out of phase in Stage I.

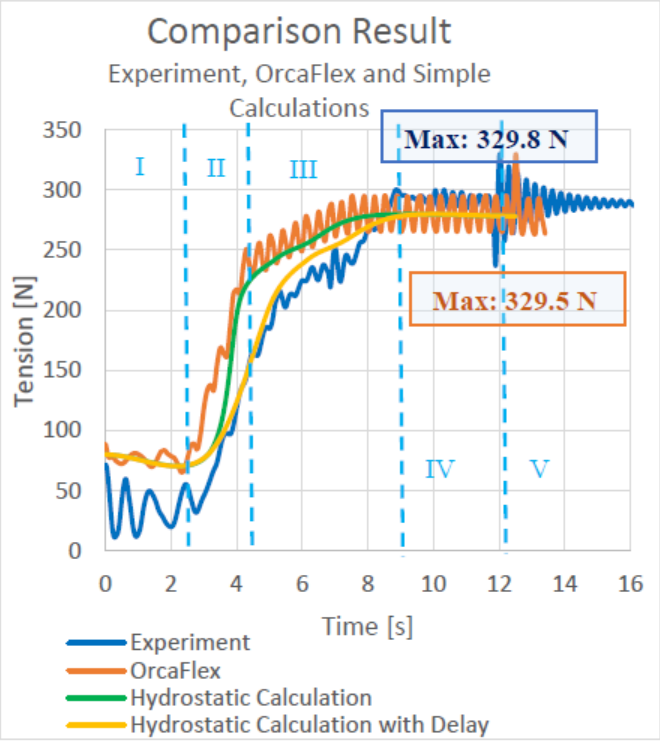

Figure 11. Tension in winch as a function of time for different simulation methods

Based on these results, we can see that the load can be divided into the hydrostatic component and wave induced component. In these cases, the hydrostatic component dominates during the recovery. As the ROV is lifted the geometric shape changes which leads to the change in submersed volume. As the main geometric shape changes, the gradient of the tension curve also changes. The wave induces a relatively small degree of fluctuation; it reduces throughout the recovery because it starts being damped. The peak value at the starting and the ending of the simulation depends on the winch acceleration and deceleration, which is also related to the recovery speed.

Because only two speeds were considered in this project, it is difficult to conclude if wire slacking is related to the change in recovery speed. It is recommended for future work to consider more speeds.

Some findings are consistent with the findings of past studied by Sayer (2008), which are:

1. The hydrodynamics loading is independent from wave frequency.
2. Wire slacking is more likely to happen when the ROV is still fully submerged rather than when it is partially out of water. Slacking is also more likely to happen in higher wave height conditions.
3. Higher order calculations did not improve the prediction accuracy.
4. Load respond delay and the phase different seen to be appear in experiment testing..

OrcaFlex gave conservative result with factor -0.2 to 0.8 offset when compared with experiment testing throughout the whole simulation. It over-estimated at the beginning because the hydrodynamics mass is assuming it is the fully submersed mass and constant throughout the whole simulation. It is under-estimated at the end because of bad modelling on the two tracks, modification on this is strongly recommended.

Wind and current forces are not considered therefore no significant drag force occur in the experiment testing. In additional, H/D and $\pi D/\lambda$ region for this experiment suggested that drag force can be ignored.

4.2 Study Two - Effect of winch wire stiffness on the ROV motion

Tests were completed over a range of frequencies for three spring stiffness':

- Spring A: Soft. K=0.48N/mm;
- Spring B: Medium. K=1.29N/mm;
- Spring C: Hard. K=2.52N/mm.

The peak response amplitude operators (RAO) were calculated from the resulting Qualisys data. Figures 12, 13 and 14 compares the response of each spring at two different water levels Figure 11, with the relatively soft spring A, the response of the ROV did not differ significantly. In Figures 12 and 13, with increasingly stiffer springs, it is clearly seen that there was a significant reduction in response motion. In figure 12, the response pattern seems to resemble phase shift towards higher frequency. However, due to the limited time available for tests, there was no data for full scale 4.05m submerged depth in lower frequency <0.5Hz to give a definite trend comparison. Figure 13 does not have enough data to draw any conclusion about the changes of response pattern.

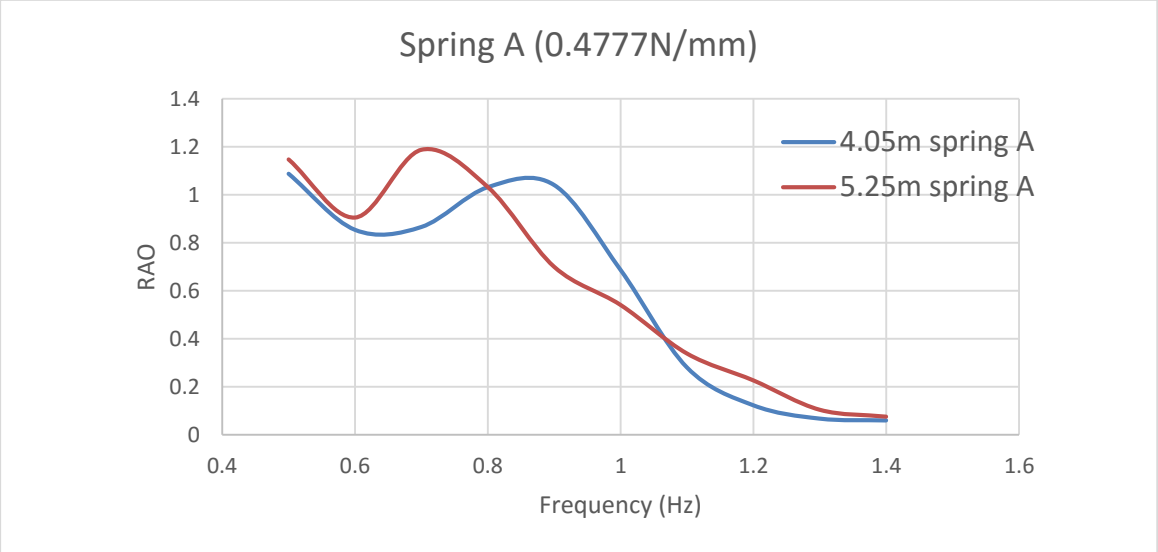

Figure 12. Measured RAO of the ROV for different depths – Spring A

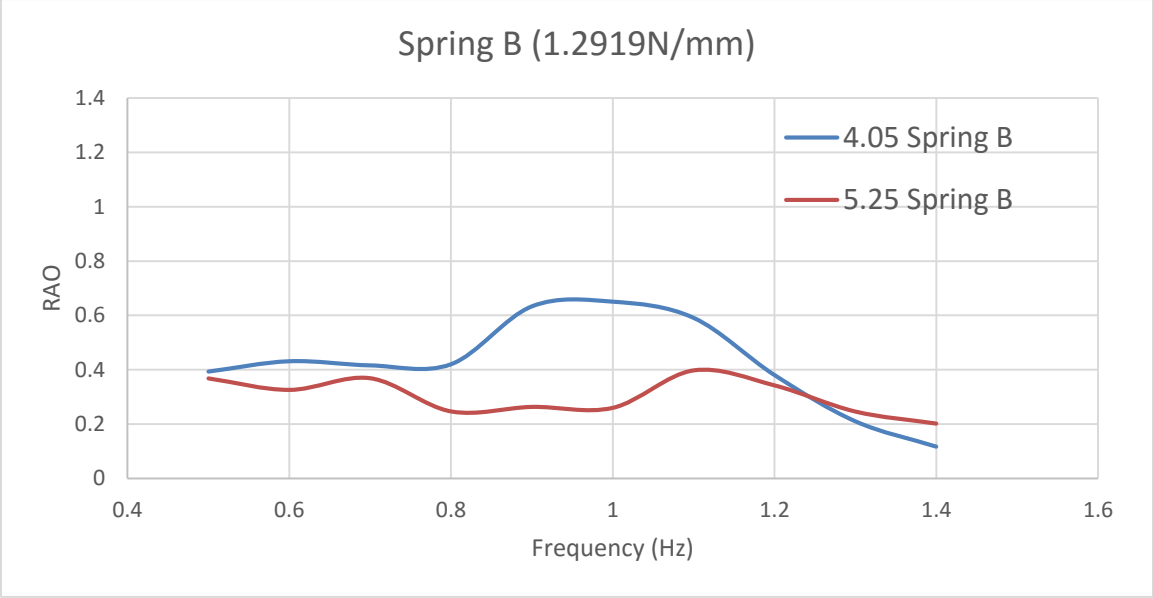

Figure 13. Measured RAO of the ROV for different depths – Spring B

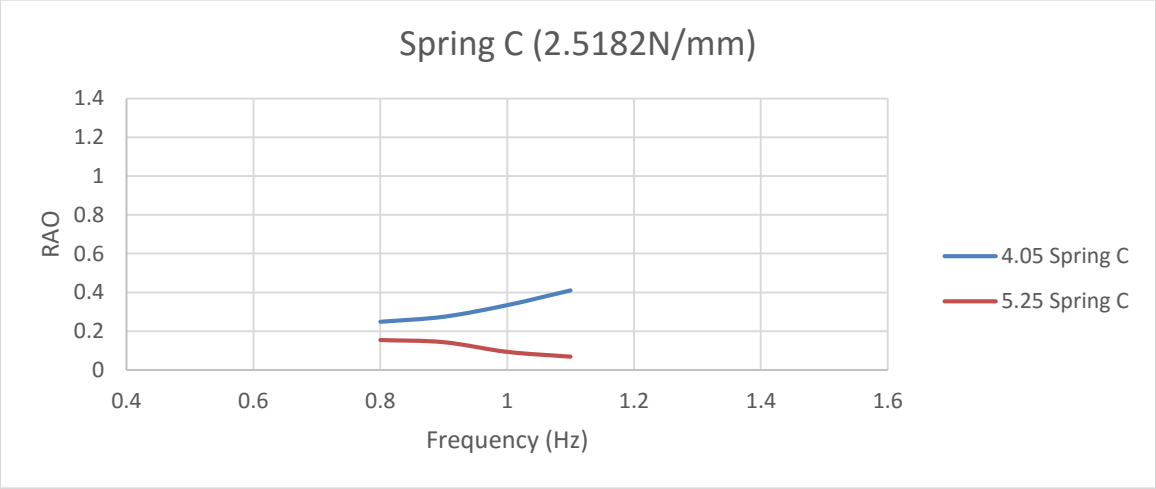

Figure 14. Measured RAO of the ROV for different depths – Spring C

Figure 12 and 13 shows clearly that at low frequency, for spring A, the RAO is approximately at 1.1 and for spring B, the RAO is approximately at 0.4. At high frequency the RAOs reduce to a low magnitude.

Figure 15 shows how response changes with increasing spring stiffness at the full scale 4.05m submerged depth. Increasing spring stiffness shows both an overall decrease in magnitude of response, and also a phase shift towards higher frequency of the response pattern.

Figure 16 shows how response changes with increasing spring stiffness at the full scale 5.25m submerged depth. At 5.25m submerged depth, increasing spring stiffness shows an overall decrease in magnitude of response. Due to the limited range of results, particularly for spring C, there is no clear trend to how the response pattern changed.

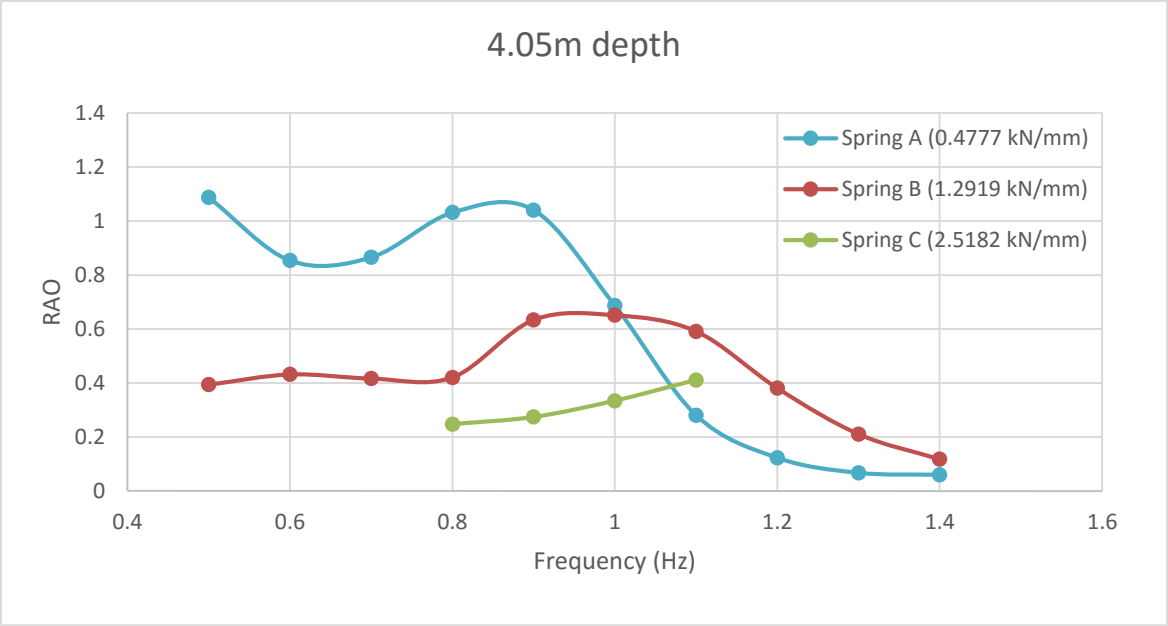

Figure 15. Measured RAO of the ROV for different spring stiffness – 4.05m depth

Spring	Peak Magnitude (RAO)	Frequency (Hz)
A	**1.0405**	**0.9**
B	**0.6509**	**1.0**
C	**0.4107***	**1.1**

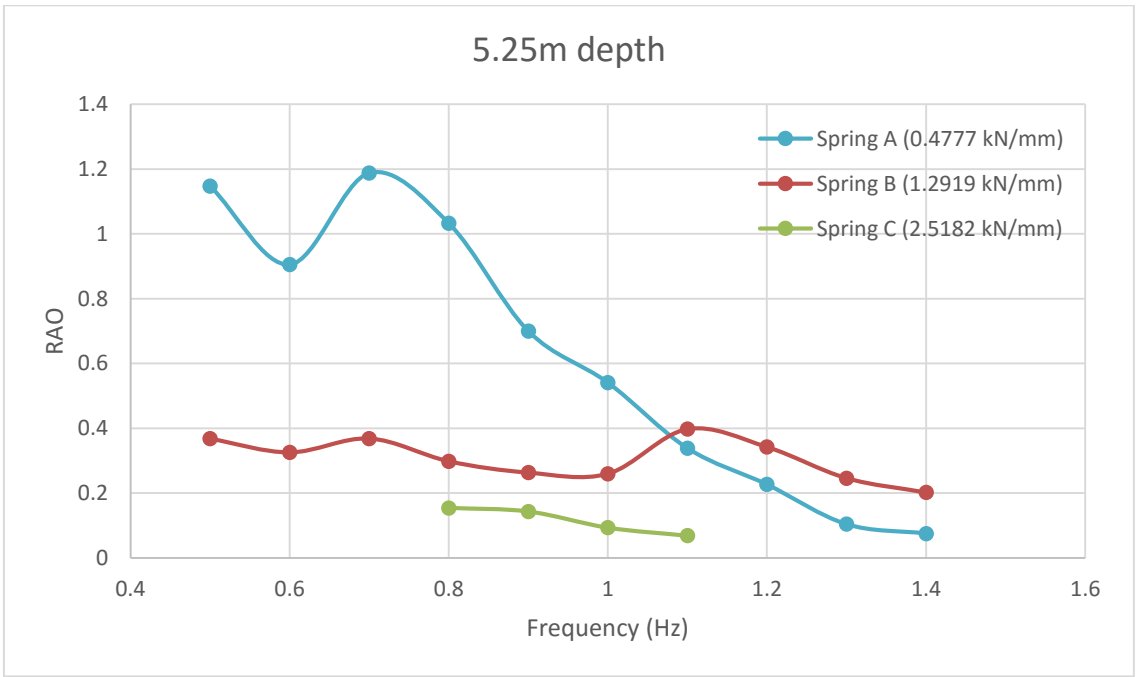

Figure 16. Measured RAO of the ROV for different spring stiffness – 5.25m depth

Spring	Peak Magnitude (RAO)	Frequency
A	**1.1876**	**0.7Hz**
B	**0.3974**	**1.1Hz**
C	**0.1539**	**0.8Hz**

Based on the results, we can see that there is a correlation between spring stiffness and the magnitude of the response. Increasing spring stiffness will cause a decrease in the magnitude of response. However, it should be noted that the response at high frequency is similar regardless of spring stiffness. The results do not give a complete understanding on how the spring stiffness affects the response pattern. From 4.05m submerged depth, it shows a phase shift of peak response towards higher frequency. It is not clear if this is reflected in 5.25m submerged depth.

The data set for Spring C is small. It is recommended for future work to obtain the complete set of data for spring C so that useful comparison can be made. It is also recommended to expand data range for Spring A to below 0.5Hz, so that there can be a definite proof that there was a phase shift towards higher frequency for 4.05m submerged depth with increasing spring stiffness. A larger number of different spring stiffness should also be tested to allow the effects of spring stiffness on the magnitude of response to be quantified.

4.3 Study Three - Damping characteristics of the ROV

Decay tests were completed for both box model and ROV. From the decay tests, decay rate and natural period can be calculated based on Faltinsen's method [6]. Decay rate is the logarithmic decrement of the amplitudes for two adjacent oscillations, while natural period is derived from the total time and number of oscillations.

Figures 17 and 18 shows the decay rate and natural period respectively for the box model. The results show the same trends for both decay rate and natural period in heave. Results compare well to the previous study completed by Bashir et al [3]. The decay rate reduces with the increment in water depth, while the natural period of the body increases. Both decay rate and natural period are almost linear to the submerged depth. The linearity is probably due to the uniform waterplane area of the box model. The gradient implies that decay rate and natural period are dependent on other particulars related to depth, for example the underwater volume and mass of the body.

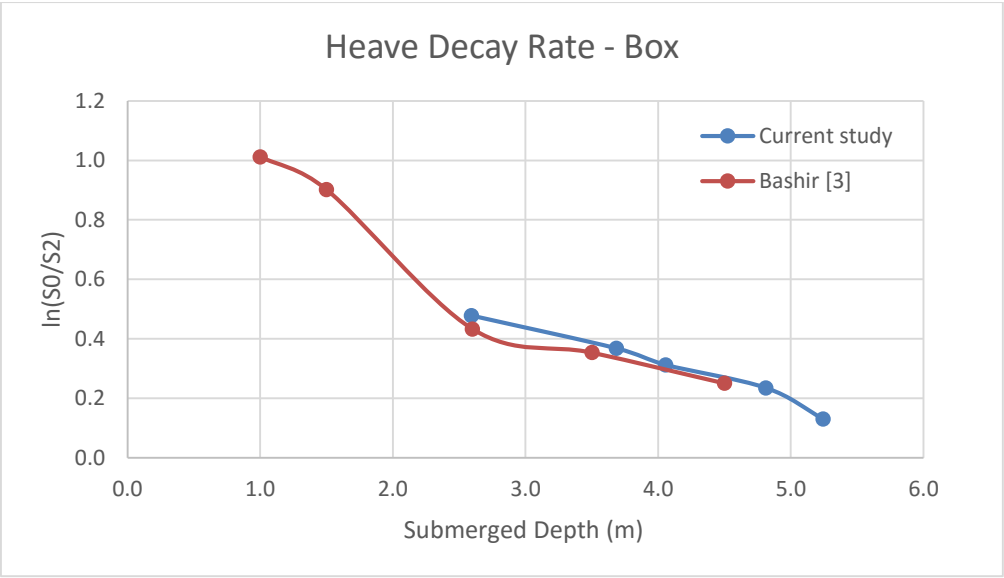

Figure 17. Heave decay rate – Box model

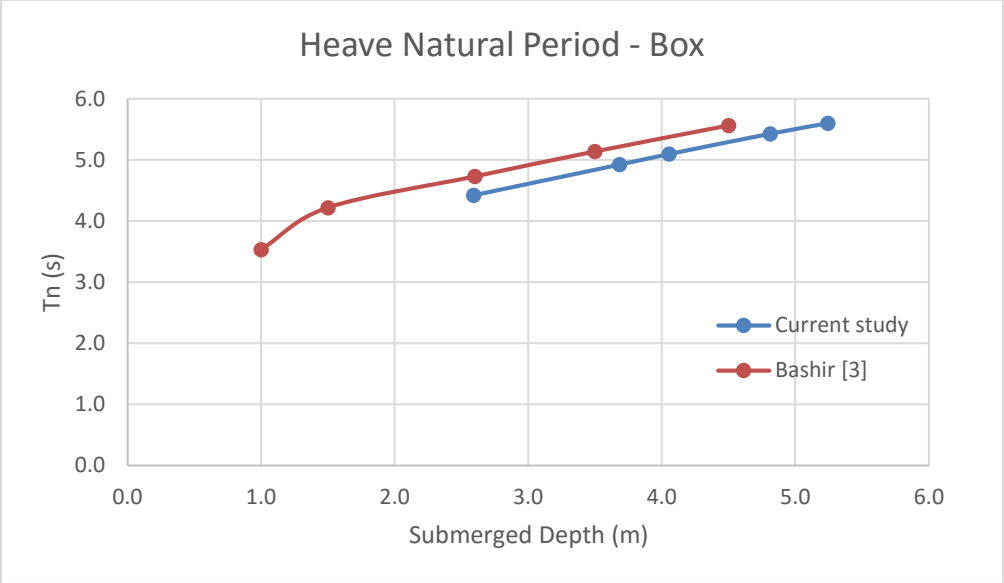

Figure 18. Heave natural period – box model

Figure 20 is a comparison of the heave decay rate between the box model and ROV. Due to the complex geometry of the ROV (as shown in Figure 19), the water plane area is different for each submerged depth. This results in a significant change in the decay rate over the range of depths tested. Less water plane area results in less restoring coefficient (Figure 21), which makes larger decay rate. This results in a nonlinear relationship between depth and decay rate. It should be noted that the submerged depth of 2.5m may have been affected by the addition of buoyancy material on the top part of the tracks.

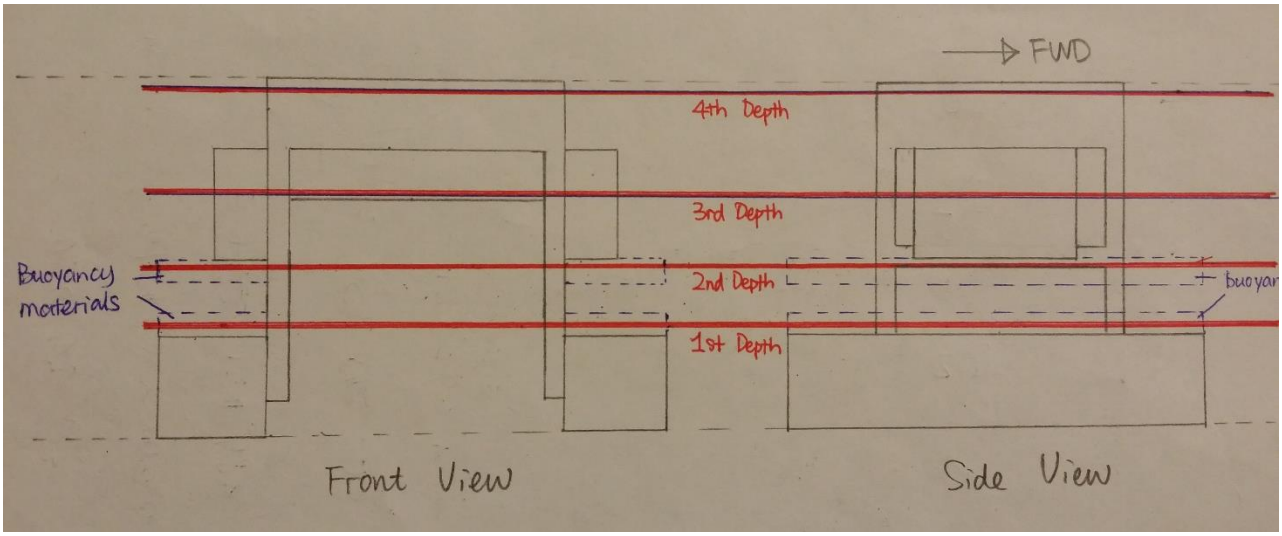

Figure 19. Sketch of the ROV measured depths showing change in waterplane area

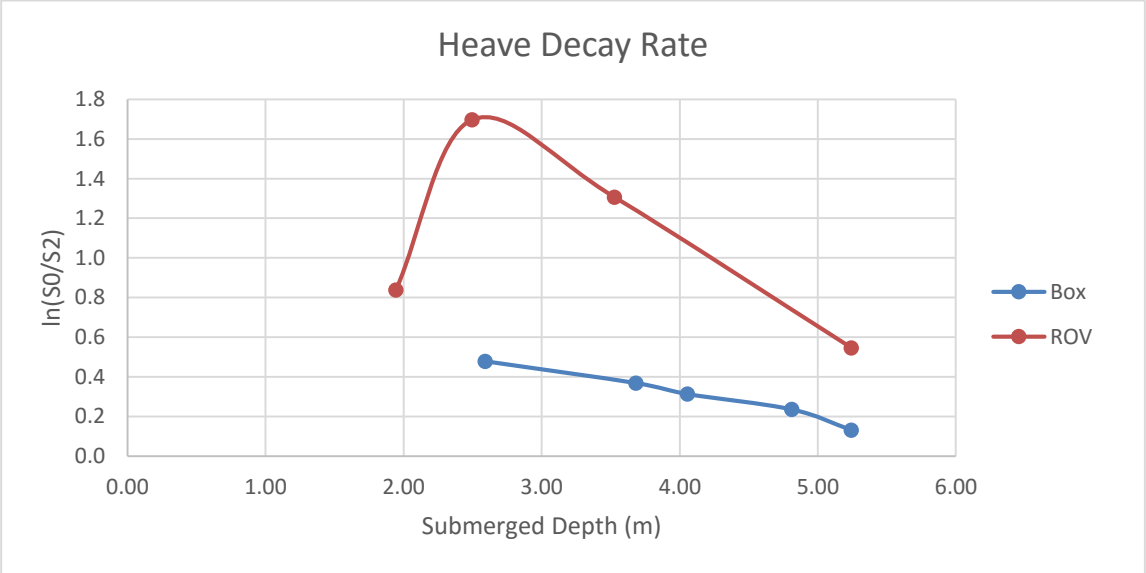

Figure 20. Heave decay rate – comparison of box and ROV

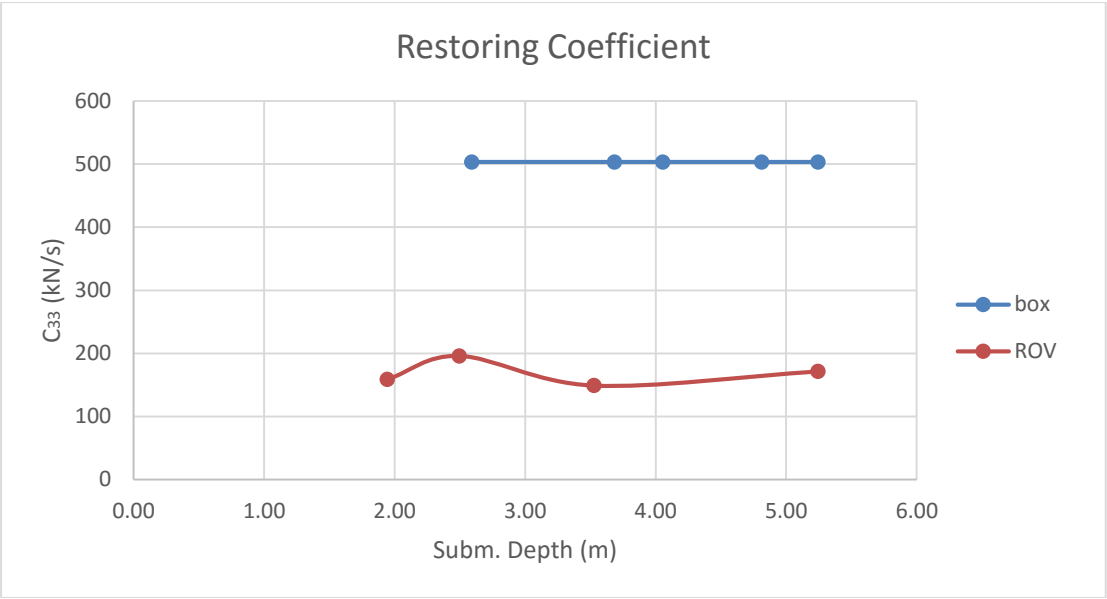

Figure 21. Restoring coefficient – comparison of box and ROV

Figure 22 illustrates the natural period for the two tested body. The linear relationships suggests that the natural period of tested body only depends on the submerged depth.

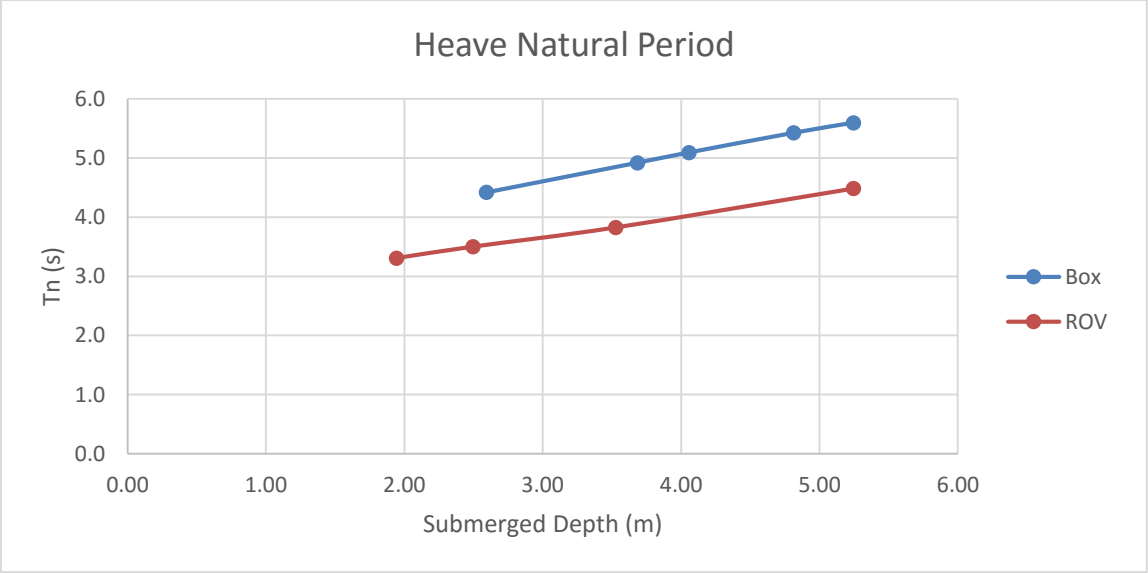

Figure 22. Heave natural period – comparison of box and ROV

Once decay rate and natural period were calculated, the damping coefficient could be derived from the equation below:

$$B = \frac{1}{\pi}\ln\left(\frac{S_0}{S_2}\right)\sqrt{C(M+A)} \quad (N/(m/s))$$

Where:

$ln\frac{S_0}{S_2}$ is the logarithmic decrement of amplitude of oscillation
C is the restoring coefficient (N/m)
M is the mass of the model (kg)
A is the added mass which is calculated as:

$$A = \frac{T_n^2}{4\pi^2}C - M\ (kg)$$

Tn is the natural period of the model (s)

These results are presented in Table 1 & 2. The damping value is shown to vary markedly over the range of submerged depths tested. The relationship with submerged depth follows a similar trend to the decay rate.

Box model						
	Heave Decay Rate	Heave Natural Period	mass	Restoring Coefficient	Added Mass	Damping value
Subm. Depth (m)	ln(S0/S2)	Tn (s)	m (t)	C_{33} (kN/m)	A_{33} (t)	B_{33} (kN/(m/s))
2.592	0.478	4.420	132.985	503.310	116.053	53.860
3.684	0.368	4.921	189.010	503.310	119.757	46.160
4.056	0.312	5.094	208.096	503.310	122.776	40.549
4.812	0.235	5.426	246.883	503.310	128.483	32.475
5.244	0.130	5.598	269.047	503.310	130.443	18.594

Table 1

ROV						
	Heave Decay Rate	Heave Natural Period	mass	Restoring Coefficient	Added Mass	Damping value
Subm. Depth (m)	ln(S0/S2)	Tn (s)	m (t)	C_{33} (kN/m)	A_{33} (t)	B_{33} (kN/(m/s))
1.944	0.837	3.307	19.181	158.986	24.870	22.300
2.496	1.608	3.501	19.181	196.053	41.672	55.900
3.528	1.306	3.826	19.554	149.096	35.735	37.734
5.244	0.546	4.484	41.645	171.470	45.679	21.250

Table 2

5. Conclusions

The three experimental studies have contributed to improving knowledge of how an ROV behaves when in the splash zone region during launch and recovery. The motion of an ROV and the resultant loading on the winch is important for the design and operation of the handling system.

Study 1 demonstrates the distinction between hydrostatic and hydrodynamic loads on the winch wire. At low wave amplitudes, such as those used in these experiments, the hydrostatic loads dominate. However, with higher wave heights, the dynamic motion of the ROV may lead to slacking in the winch wire and undesirable peak loads. Furthermore, the acceleration and deceleration of the winch at the beginning and end of the simulation respectively can result in sharp peak loads. These may be particularly concerning with the ROV fully submerged as they may cause snatching of the wire. The study shows that the recovery speed is also an important factor. Relatively fast speeds were tested in this study, which means that the ROV is recovered within a couple of wave periods. Further work at slower, more realistic, recovery speeds may be needed to better capture the influence of wave action on the ROV motion and resulting winch line forces.

Study 2 derives RAO plots of the ROV at different heights within the splash zone, replicating previous experimental method by the same research team [3]. These experiments, and the resulting RAOs, serve two purposes. Firstly, they give a direct assessment of the influence of winch wire stiffness on the ROV motion. This study has shown that increasing winch wire stiffness decreases motion. Secondly, the RAOs can be used to derive hydrodynamic coefficients for the ROV which could be used in a hydrodynamic modelling tool such as OrcaFlex. For this purpose, the softer spring results are considered more appropriate because they should better isolate the ROV from the influence of the winch. This means comparison can be made to equivalent hydrodynamic models of the ROV in isolation. This has previously been shown to be successful by Bashir et al [3]. The results presented here confirm that the spring stiffness is important to consider, and in particular that a stiffer spring will influence the motion behaviour. Further tests are still needed to fully determine if the softest spring used here is completely isolating the ROV.

Study 3 calculates the damping value of the ROV model in different positions relative to the water surface. The KTP project, for which this study forms a part, has determined that damping is critical for adequately defining the motion of the ROV in the splash zone using a numerical tool such as OrcaFlex. The results in this study show that the damping value changes markedly as the ROV emerges through the water surface. This is an important finding because it shows that damping must be carefully controlled in a numerical simulation. At present a lumped mass hydrodynamic model such as may be used in OrcaFlex is defined with a single damping value. This may cause inaccuracy in a launch and recovery simulation. Further work should be undertaken to clarify the damping value for an ROV over a complete range of submerged depths and then enable this to be modelled explicitly in a numerical simulation.

All three studies here have only considered the motion of the ROV connected to a rigidly positioned winch. In reality, a launch or recovery process at sea will also be influenced by the motion of the deployment ship. Software tools such as OrcaFlex are ideal for simulating this type of scenario. However, much care needs to be taken to adequately define the hydrodynamic properties of the ROV in a simulation. All three studies presented in this paper demonstrate the complex hydrodynamic behaviour of the ROV when located in the splash zone. This behaviour can be modelled only by using

reasonable parameters for added mass and damping. These parameters can change quite markedly as the ROV emerges through the water surface. This means that coefficients to describe added mass and damping need careful control during a simulation of a launch or recovery process.

6. Acknowledgements

The supervising authors would like to thank SMD for their kind support of the students whilst completing these projects, and for hosting several tours of the ROV manufacturing facilities. Thanks in particular to Daniel Cunny, Rob Eastwood, Michael van Zwanenberg and Mahesh Menon.

Kang Tay and Bingbing Ke have been supported by Newcastle University Vacation Scholarships. The recovery simulations formed part of a final stage dissertation submitted by Clandia Sim.

This work complements a Knowledge Transfer Partnership (KTP) project between Newcastle University and Soil Machine Dynamics, with funding from Innovate UK. The project team would like to thank Jon Dean from Innovate UK and the KTP support office at Newcastle University.

6. References

[1] Y. Bai and Q. Bai, *Subsea Engineering Handbook*. Gulf Professional Publishing, 2012.
[2] P. Sayer, 'Hydrodynamic loads during the deployment of ROVs', *Ocean Eng.*, vol. 35, no. 1, pp. 41–46, Jan. 2008.
[3] M. Bashir, S. Benson, A. Murphy, M. Menon, R. Eastwood, D. Cunny, and M. Zwanenberg, 'Hydrodynamic Characteristics of ROVs During Deployment Through Wave-Affected Zone', in *34th International Conference on Ocean, Offshore and Arctic Engineering (OMAE)*, 2015.
[4] I. A.T. Morrison and D. R. Yoerger, 'Determination of the hydrodynamic parameters of an underwater vehicle during small scale, nonuniform, 1-dimensional translation', in *OCEANS '93. Engineering in Harmony with Ocean. Proceedings*, 1993, pp. II277–II282 vol.2.
[5] Eng Y.-H., Lau M.-W., and Chin C.-S., 'Added Mass Computation for Control of an Open-Frame Remotely-Operated Vehicle: Application Using WAMIT and MATLAB', *J. Mar. Sci. Technol.*, no. 預刊文章, pp. 1–12, Mar. 2013.
[6] O. Faltinsen, *Sea Loads on Ships and Offshore Structures*. Cambridge University Press, 1993.